

# Effect of Thermal Radiation and Radiation absorption on Hydromagnetic convective Heat and Mass transfer flow of a Jeffrey Fluid in a Concentric Cylindrical Annulus

Dr. Palla Kristaiah

*Assistant Professor, Department of Mathematics, A.P.J. Abdul Kalam III-T, Ongole, R.K. Valley Campus, Idupulapaya, Y.S.R. Kadapa (Dt), Andhra Pradesh, India*

**Abstract:** An attempt has been made to discuss the coupled effect of thermal radiation, radiation absorption heat sources on convective heat and mass transfer flow of Jeffrey fluid in annular region in concentric cylinders with non-linear density temperature relation. The coupled governing equations have been solved by Finite element technique with quadratic functions. It has observed that higher thermal radiation ( $R_d$ ) enhances with  $R_d < 1.5$  and reduces with  $R_d > 3.5$ . Higher the radiation absorption ( $Q_1$ ) larger the velocity.

**Keywords:** Thermal radiation, Radiation absorption, Heat sources, chemical reaction, non-linear density temperature relation.

## 1. INTRODUCTION

The study of non-Newtonian fluids has been focusing on several investigations during the past few decades because of its extensive engineering and industrial applications. Especially, the industries and engineering, polymer solutions and in polymer melt in the plastic processing, non-Newtonian fluids and heat transfer can also play central role in food engineering, petroleum production also. Mahanta and Shaw [15] investigated the MHD Casson fluid flow over a linearly stretching porous sheet with convective boundary. Hsiao [13] investigated mixed convection heat transfer problem of a second-grade MHD viscous elastic fluid past a wedge in porosity with suction or injection. Wang [36], Labropulu and Li [14] studied the effect of slip flow of a non-Newtonian fluid behaviour at a stagnation-point over a plate. Ramachandran et al., [23] discussed the consequent flow and heat transfer characteristics that are also brought about by the stretching sheet with power-law velocity variation. Abel and Mahesha [1] examined the effects of MHD flow of a non-Newtonian viscoelastic fluid over a stretching sheet in the presence of non-uniform radiation and heat source.

The effects of thermal radiation and porosity on MHD mixed convection flow in a vertical channel using homotopy analysis method are also carried out by Srinivas and Muthuraj [32]. Rosca and Pop [25] studied the steady forced flow and convection heat transfer over a vertical shrinking/stretching sheet with the help of slip condition. Andersson [2] investigated the slip-flow of a viscous fluid past a linearly stretching sheet. It is found out that the assumption of the convective no-slip condition at the boundary is not always factual and hence should be substituted by partial slip boundary conditions in particular situations. Chaudhary and Kumar [5] did analysis on the steady electrically conducting 2-D boundary-layer flow of an incompressible fluid near a stagnation-point past a shrinking sheet with slip conditions. Recently Ming Shen et al., [17] studied on MHD mixed convection viscous flow near a stagnation-point area over a non-linear stretching sheet with velocity slip and specified surface heat flux. Radiation is the process by which heat energy is transmitted from one place to another without the aid of any material medium. When a body is hotter, the energy of vibration of the atoms and molecules is sent out from it in the form of radiant heat waves. These waves which are falling on another body induce the molecules to vibrate there and hence the body is heated up. In many fluid-particle flows, thermal radiation effects play an important role in altering the heat transfer characteristics. Muthucumaraswamy and Visalakshi [18] studied radiative flow and heat transfer past an exponentially accelerated vertical plate with uniform mass diffusion.

A large class of real fluids does not exhibit the linear relationship between stress and the rate of strain. Because of the non-linear dependence, the analysis of the behavior of the fluid motion of the non-Newtonian fluids tends to be much more complicated and subtle in comparison with that of the Newtonian fluids. It is well known that the rheological properties of many fluids are not well modeled by the Navier-Stokes equations. That is why several models of non-Newtonian fluids are proposed. Jeffery- six constant fluids is one of these models. It is not possible to obtain a single equation exhibiting all properties of all non-Newtonian fluids from available literature. In the literature, the mechanics of non-linear fluids presents special challenges to engineers, physicists and mathematicians since the non-linearity can manifest itself in a variety of ways.

Free convection flow and heat transfer in hydromagnetic case is important in nuclear and space technology (Ganapathy [8], Nanda [19], Neeraja [20], Osterle [21], Roots [24], Vasudev [35]). Chen and Yuh

[6] have investigated the heat and mass transfer characteristics of natural convection flow along a vertical cylinder under the combined buoyancy effects of thermal and species diffusion. Philip [22] has obtained analytical solution for the annular porous media valid for low modified Reynolds number Antonio [3] has investigated the laminar flow, heat transfer in a vertical cylindrical duct by taking in to account both viscous dissipation and the effect of buoyancy..

In all the above investigations, the variation of density is taken in the linear form

$$\Delta\rho = -\rho\beta(\Delta T)\dots \quad (A)$$

Where  $\beta$  is the co-efficient of thermal expansion and is  $2.07 \times 10^4 (\text{OC})^{-1}$ . This is valid for temperature variation near  $20^\circ\text{C}$ . But this analysis is not applicable to the study of the flow of water at  $4^\circ\text{C}$ , the density of water is maximum at atmosphere pressure and the above relations (A) does not hold good. The modified form of (A) is applicable to water at  $4^\circ\text{C}$  is given by

$$\Delta\rho = -\rho\gamma(\Delta T)^2 \dots \quad \dots(B)$$

where  $\gamma = 8 \times 10^{-6} (\text{OC})^{-2}$ . Taking this fact into account, Goren [10] showed in this case, similarity solutions for free convection flow of water at  $4^\circ\text{C}$  past a semi-infinite vertical plate. Govindarajulu [11] showed that a similarity solution exists for the free convection flow of water at  $4^\circ\text{C}$  from vertical and horizontal plates in the presence of suction and injection. Gupta, Dubey and Sharma [12] have discussed the laminar free convection flow through coaxial circular cylinders with and without heat sources. Soundalgekar [30] obtained an approximate solution of the same problem using Kraman – Pohlhausen integral method. Taking non-linear density temperature variation Sarojamma [26] has analysed the hydromagnetic free convection flow in a cylindrical geometry. Datta [7] has investigated the free convection of water at  $4^\circ\text{C}$  from a horizontal plate when wall temperature varies as a power of distance along the plate. An approximate solution for velocity and temperature has been obtained by using Karman – Pohlhausen method together with the method of finding similarity solution. Using the relation (B) Sinha [29] has analyzed the problem of fully developed free convection flow between vertical plates in a circular pipe. Sastri and Vajravelu [27] have solved the problem of free convection between vertical walls by taking the non-linear density temperature variation, viz.,

$$\Delta\rho = -\rho\beta_0(T - T_e) - \rho\beta_1(T - T_e)^2 \dots \quad (C)$$

where  $\beta_0$  and  $\beta_1$  are constants. This relation includes both the relationships (A) and (B). Gilpin [9] has used a density temperature relation which is similar to relation (C) and has shown the existence of Quasi – steady modes of convection for some temperature below  $4^\circ\text{C}$ . A similar relation introduced by Varrier and Tien [34] has been used to predict the heat transfer results in the case of water for temperature between  $0^\circ\text{C}$  and  $20^\circ\text{C}$ . Bhargawa and Agarwal [4] have investigated the fully developed laminar free convection flow in the presence of constant heat source in a circular pipe taking the same density temperature relationship (C). It is found that the flow and heat transfer both depends up on a new parameter  $\gamma = \left(\frac{\beta_1}{\beta_0}\right)\Delta T$  in addition to the heat source parameter and free convection parameter k.

The effect of heat transfer on MHD oscillatory flow of a Jeffrey fluid in a channel with slip effect at lower wall. The effects of various emerging parameters on the velocity and temperature are discussed through graphs in detail. Vasudev et al [35] have discussed the effect of Heat Transfer on the peristaltic flow of a Jeffrey Fluid through a Porous medium in a vertical Annulus. Sreenath et.al [20] has investigated the effect of quadratic density temperature variation on convection heat transfer flow of a Jeffrey fluid in a tube and circular annulus. Recently Madhusudhana Reddy [16] has investigated Jeffrey fluid flow a concentric annulus under radial magnetic field.

In this paper, we analyzed the effect of thermal radiation, radiation absorption, non-linear density temperature variation on hydromagnetic mixed convective heat and mass transfer flow of a Jeffrey's fluid through a porous medium in a circular annulus in the presence of temperature dependent heat source. The equations governing the flow, heat and mass transfer have been solved by employing Finite element method. The effect of various governing parameters on the flow characteristics have been discussed graphically. The skin friction, rate of heat and mass transfer are evaluated numerically for different variations.

## 2. FORMULATION OF THE PROBLEM

We investigate the fully developed steady laminar free convective flow of a viscous, electrically conducting Jeffrey fluid through a porous medium confined in an annular region between two vertical co-axial porous circular pipes in the presence of heat generating sources. We choose the cylindrical polar coordinates system  $O(r, \theta, z)$  with the inner and outer cylinders at  $r = a$  and  $r = b$  respectively. The fluid is subjected to the influence of a radial magnetic field  $(H_0 / r)$ . Pipes being sufficiently long, all the physical quantities are independent of the axial coordinate  $z$ . Assuming the

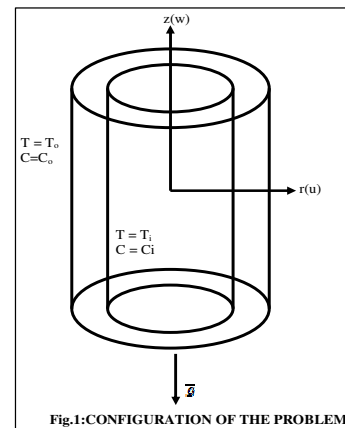


Fig.1: CONFIGURATION OF THE PROBLEM

magnetic Reynolds number to be small we neglect the induced magnetic field in comparison to the applied magnetic field. Also the motion being rotationally symmetric the azimuthal velocity  $V$  is zero. The equations governing free convective heat and mass transfer flow under no pressure gradient are

$$w_{rr} + (1 - a u_a / \nu) w_r / r + ((\beta_0 g / \nu) (T - T_e) + (\beta_1 g / \nu) (T - T_e)^2 + (\beta^* g / \nu) (C - C_e)) - (\sigma \mu_e^2 H_0^2 a^2 / \nu (1 + \lambda_1)) (w / r^2) - (\nu / k (1 + \lambda_1)) w = 0 \quad (1)$$

$$T_{rr} + (1 - a u_a / \nu) T_r / r + (Q / k_f) + \frac{Q_1}{k_f} (C - C_e) - \frac{1}{r} \frac{\partial (r q_R)}{\partial r} = 0 \quad (2)$$

$$C_{rr} + (1 - a u_a / \nu) C_r / r - \left( \frac{k_c}{D_B} \right) C = 0 \quad (3)$$

Using Rosseland approximation and introducing the non-dimensional variables as  $(r', w', \theta')$   
 $r' = r/a$ ,  $w' = w(a/\nu)$ ,

$$\theta = \frac{T - T_e}{T_i - T_e}, C' = \frac{C - C_e}{C_i - C_e} \quad (4)$$

the equations (1)–(3) reduce to

$$w_{rr} + (1 - \lambda) (1/r) w_r - (D^{-1} + (M^2 / (1 + \lambda_1)) r^2) w = -(G / (1 + \lambda_1)) (\theta + \gamma_1 \theta^2 + N C) \quad (5)$$

$$(1 + \frac{4Rd}{3}) \theta_{rr} + (1 - \lambda P) \theta_r / r - \alpha \theta + Q_1 C = 0 \quad (6)$$

$$C_{rr} + (1 - \lambda Sc) C_r / r - (\gamma Sc) C = 0 \quad (7)$$

where

$M = (\sigma \mu_e^2 H_0^2 a^2 / \rho \nu)^{1/2}$  (Hartmann number),  $G = (\beta g a^3 (T_i - T_e)^2 / \nu^2)$  (Grashoff number),

$\lambda = a u_a / \nu$  (Suction parameter),  $D^{-1} = (a^2 / k)$  (Darcy parameter),  $P = (\mu C_p / k_f)$  (Prandtl number),

$\alpha = \frac{QL^2}{\Delta T k_f}$  (Heat Source parameter),  $\gamma_1 = \frac{\beta_1 \Delta T}{\beta_0}$  (non-linear density temperature ratio),

$Q_1 = \frac{Q_1 a^2 \Delta c}{k_f \Delta T}$  (Radiation absorption parameter),  $\gamma = \frac{k_1 a^2}{D_1}$  (Chemical reaction parameter),  $N = \frac{\beta^* \Delta C}{\beta \Delta T}$

(Density ratio),  $s = \frac{b}{a}$  (width of annular region)

The corresponding boundary conditions are

$$w = 0, \theta = 1, C = 1 \quad \text{on } r = 1$$

$$w = 0, \theta = 0, C = 0 \quad \text{on } r = s \quad (8)$$

### 3. FINITE ELEMENT ANALYSIS

The non-linear coupled governing equations(5-7) have been solved by using finite element method. The finite element analysis with quadratic polynomial approximation functions is carried out along the radial distance across the circular duct. The behavior of the velocity, temperature and concentration profiles has been discussed computationally for different variations in governing parameters. The Galarkin method has been adopted in the variational formulation in each element to obtain the global coupled matrices for the velocity, temperature and concentration in course of the finite element analysis.

Choose an arbitrary element  $e_k$  and let  $w^k$ ,  $\theta^k$  and  $C^k$  be the values of  $w$ ,  $\theta$  and  $C$  in the element  $e_k$

We define the error residuals as

$$E_w^k = \frac{d}{dr} \left( \left( \frac{1}{1 + \lambda} \right) r \frac{dw^k}{dr} \right) + G(\theta^k + \gamma_1 (\theta^k)^2 + N C^k) - (D^{-1} + \frac{M^2}{r^2}) r w^k \quad (9)$$

$$E_\theta^k = \frac{1}{Pr} \frac{d}{dr} \left( (1 - \lambda P) r \frac{d\theta^k}{dr} \right) - \frac{\alpha}{Pr} r \theta^k + Q_1 C^k + \frac{4Rd}{3} \frac{d}{dr} \left( r \frac{d\theta^k}{dr} \right) \quad (10)$$

$$E_c^k = \frac{d}{dr} \left( (1 - \lambda Sc) r \frac{dC^k}{dr} \right) - k_r C^k \quad (11)$$

where  $w^k$ ,  $\theta^k$  &  $C^k$  are values of  $w$ ,  $\theta$  &  $C$  in the arbitrary element  $e_k$ . These are expressed as linear combinations in terms of respective local nodal values.

$$w^k = w_1^k \psi_1^k + w_2^k \psi_2^k + w_3^k \psi_3^k, \theta^k = \theta_1^k \psi_1^k + \theta_2^k \psi_2^k + \theta_3^k \psi_3^k, C^k = C_1^k \psi_1^k + C_2^k \psi_2^k + C_3^k \psi_3^k$$

where  $\psi_1^k, \psi_2^k, \dots$  etc are Lagrange's quadratic polynomials.

Galerkin's method is used to convert the partial differential Eqs. (10) – (11) into matrix form of equations which results into  $3 \times 3$  local stiffness matrices. All these local matrices are assembled in a global matrix by substituting the global nodal values of order I and using inter element continuity and equilibrium conditions.

The shear stress ( $\tau$ ), Nusselt number (rate of heat transfer), Sherwood number (rate of mass transfer) are evaluated by using the following formulas

$$\tau = \left( \frac{dw}{dr} \right)_{r=1,1+s}, Nu = - \left( \frac{d\theta}{dr} \right)_{r=1,1+s}, Sh = - \left( \frac{dC}{dr} \right)_{r=1,1+s}$$

#### 4. PARTICULAR CASE

In the absence of radiation absorption (Q1) the results are in good agreement with that of *Suresh Babu* et. al [33].

#### 5. RESULTS AND DISCUSSION

The equations governing the flow, heat and mass transfer have been solved by numerical technique. The velocity, temperature and concentration distributions have been discussed graphically for different parametric variations. Figures 2 – 13 represents the axial velocity  $w$  for different values of  $G, M, D-1, Rd, Q1, N, \gamma, \lambda, \alpha, \lambda_1$  and  $\gamma_1$ .

The variation of velocity ( $w$ ) with Grashoff number ( $G$ ) is shown in fig.2. From the profiles we notice an enhancement in the magnitude of  $w$  with increasing values of  $G$ . The region of reversal flow enlarges with  $G$  in the region (1.5,2.0). Fig.3 represents  $w$  with magnetic parameter ( $M$ ). Higher the Lorentz force smaller the velocity in the flow region and the region of reversal flow shrinks with  $M$ . Fig.4 shows the variation of  $w$  with inverse Darcy parameter ( $D^{-1}$ ). Lesser the permeability of the porous parameter, smaller the magnitude of  $w$  in the flow region and size of the reversal flow reduce with increase in  $D-1$ . Fig.6 represents  $w$  with buoyancy ratio ( $N$ ). It can be seen from the velocity profiles that when the molecular buoyancy force dominates over the thermal buoyancy force the magnitude of the axial velocity reduces in the entire flow region irrespective of the directions of the buoyancy forces and the region of reversal flow grows in size with  $N$ . Fig.5 shows the variation of  $w$  with heat source parameter ( $\alpha$ ). We notice from the graphs that the magnitude of  $w$  reduces with increase in the strength of the heat source and reduces in the presence of heat absorption. This is due to the fact that energy is absorbed in the presence of source and generated in the presence of heat absorption. The region of reversal flow grows with increased in  $\alpha > 0$  and shrinks with  $\alpha < 0$ . The effect of thermal radiation ( $Rd$ ) on  $w$  can be seen from fig.9. We find that higher the thermal heat flux ( $Rd < 1.5$ ) larger the velocity in the annular region and for higher  $Rd > 3.5$ , we notice a depreciation in the velocity and the region of reversal flow reduces with increase in  $Rd$ . The effect of chemical reaction ( $\gamma$ ) on  $w$  can be seen from fig.10. The magnitude of  $w$  enhances in the region (1,1.5) and reduces in the region (1.5,2.0) in both degenerating /generating cases in the region. The region of reversal flow reduces with increase in  $\gamma$ . From fig.8 we find that an increase in the suction parameter ( $\lambda$ ). We observe that higher the suction parameter  $\lambda$  larger  $|w|$  in the flow region. The region of reversal flow grows in size with increase in  $\lambda$ . The effect of Schmidt number  $Sc$  on  $w$  can be seen from Fig (7). It can be seen that lesser the molecular diffusivity smaller  $|w|$  in the flow region (1, 1.5) and larger in the region adjacent to the outer cylinder. The region of reversal flow shrinks with increase in  $Sc$ . The effect of radiation absorption (Q1) on  $w$  can be seen from fig.8. We find that higher the radiation absorption effects larger the magnitude of  $w$  in the flow region and region of reversal flow increases with increase in Q1. The effect of suction parameter ( $\lambda$ ) on  $w$  can be seen from fig.11. From the profiles we find that the magnitude of  $w$  enhances in the region (1,1.6) and in the region (1.6,2) it reduces with increase in suction parameter ( $\lambda$ ). The region of reversal flow shrinks with  $\lambda$ . The effect of Jeffrey parameter ( $\lambda_1$ ) on  $w$  can be seen from Fig (12). It is found that  $|w|$  experiences an enhancement in the region (1,2) and the region of reversal flow increases with  $\lambda_1$  in the entire flow region. Fig (13) represents the effect of non-linear density temperature variation ( $\gamma_1$ ). It is found that the non-linearity in the density – temperature variation results in an enhancement in  $|w|$  in the flow region (1,2) and the region of reversal flow grows with increase in  $\gamma_1$ .

The non-dimensional temperature distribution ( $\theta$ ) is shown in Figs. 14-19 for different parametric variations. We follow the convention that the non-dimensional temperature convection is positive or negative according as the actual temperature ( $T$ ) is greater / lesser than equilibrium temperature ( $T_e$ ).

Fig (14) represents  $\theta$  with heat source parameter ( $\alpha$ ). The actual temperature enhances with increase in  $\alpha > 0$  and reduces with  $|\alpha|$  ( $\alpha < 0$ ). From Fig (15) we notice that the actual temperature enhances in the flow region (1,2) with increase in  $Sc$ . Also higher the radiation absorption (Q1) smaller the actual temperature in the flow region (1,2) (fig.16). Higher the Radiation heat flux smaller actual temperature in the flow region (Fig.17). The effect of chemical reaction  $\gamma$  on  $\theta$  can be seen from Fig (18). It can be seen from the profiles that the actual

temperature reduces in both the degenerating /generating chemical reaction cases. The effect of porosity of the boundary  $\lambda$  can be observed from Fig (19). It is found that higher the suction parameter at the boundary larger the actual temperature in the flow region (1,1.5) and smaller in the region(1.5,2.0).

The non-dimensional concentration (C) is exhibited in figures 20-22 for different parametric values. We follow the convention that the non-dimensional concentration is positive or negative according as the actual concentration is greater/ lesser than the equilibrium concentration ( $C_\infty$ ).

The actual concentration enhances in the region (1,1.4) and reduces in the region(1.5,2.0) with increase in Sc (Fig 20 ). Fig (21) represents the concentration with chemical reaction parameter  $\gamma$ . It can be seen from the profile that the actual concentration reduces in the region (1,1.5) and enhances in(1.5,2.0) in both the degenerating/generating chemical reaction cases . The effect of suction parameter ( $\lambda$ ) on C can be seen from fig.22.It can be seen from the profiles that the actual concentration reduces in the region (1,1.4) and enhances in the region(1.5,2.0)with increase in suction parameter.

The shear stress, Nusselt and Sherwood numbers at the inner and outer cylinder  $r=1$  &  $r=2$  are shown in tables 2 for different parametric variations. It is found that the stress increases with increase in  $G>0$  and reduces with  $M, D^{-1}$  at  $r=1&2$ .  $|\tau|$  enhances with increase in the strength of the heat generating source and reduces with  $|\alpha|$  at the inner and outer cylinders  $r=1$  & 2. An increase in  $\alpha>0$  enhances Nu and reduces with  $\alpha<0$  at both the cylinders. When the molecular buoyancy force dominates over the thermal buoyancy force the stress enhances at  $r=1&2$  when the buoyancy forces are in the same direction and for the forces acting in opposite directions, it reduces at inner cylinder  $r=1$  and enhances at  $r=2$ . Higher the thermal radiation (Rd) larger the stress at  $r=1$  and smaller at  $r=2$ . The rate of heat transfer increases at both the cylinder with increasing values of Rd. The stress enhances at  $r=1$  and reduces at  $r=2$  with increase in suction parameter  $\lambda$ . Nu and Sh reduce at the inner cylinder  $r=1$  and enhances at  $r=2$  with suction parameter( $\lambda$ ). The stress enhances at both the cylinders  $r=1&2$  with increase in the Jeffrey parameter  $\lambda_1$ . An increase in Sc enhances the stress on  $r=1$  and reduces on  $r=2$ . The heat and mass transfer reduces at  $r=1$  and enhances at  $r=2$  with increasing values of Sc. We notice that  $|\tau|$  increases at  $r=1$  and reduces at  $r=2$  with increase in Sc .

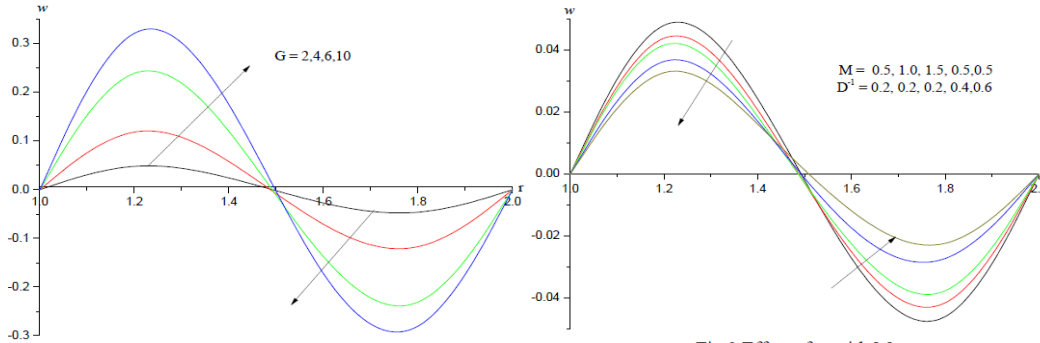


Fig.2 Effect of w with G  
M=0.5,  $D^{-1}=2$ ,  $\alpha=2$ , N=1, Sc=1.3,  
Q1=0.5, Rd=0.5,  $\gamma=0.5$ ,  $\lambda_1=0.1$ ,  $\gamma_1=0.1$

Fig.3 Effect of w with M  
G=10,  $D^{-1}=2$ ,  $\alpha=2$ , N=1, Sc=1.3,  
Q1=0.5, Rd=0.5,  $\gamma=0.5$ ,  $\lambda_1=0.1$ ,  $\gamma_1=0.1$

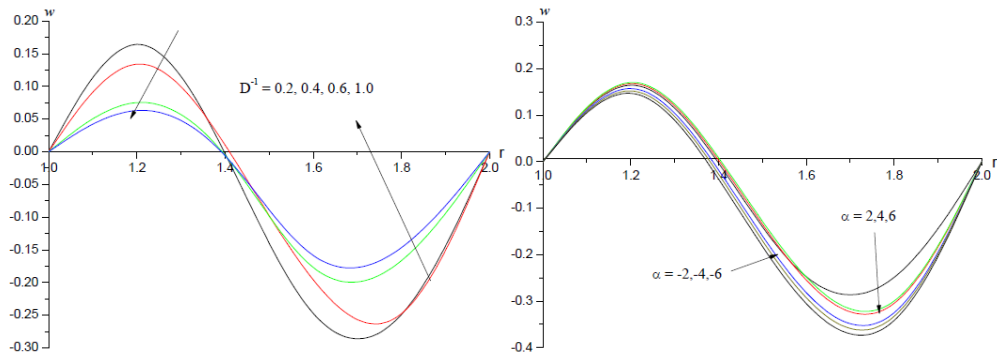


Fig.4 Effect of w with  $D^{-1}$   
G=10, M=0.5,  $\alpha=2$ , N=1, Sc=1.3,  
Q1=0.5, Rd=0.5,  $\gamma=0.5$ ,  $\lambda_1=0.1$ ,  $\gamma_1=0.1$

Fig.5 Effect of w with  $\alpha$   
G=10, M=0.5,  $D^{-1}=2$ , N=1, Sc=1.3,  
Q1=0.5, Rd=0.5,  $\gamma=0.5$ ,  $\lambda_1=0.1$ ,  $\gamma_1=0.1$

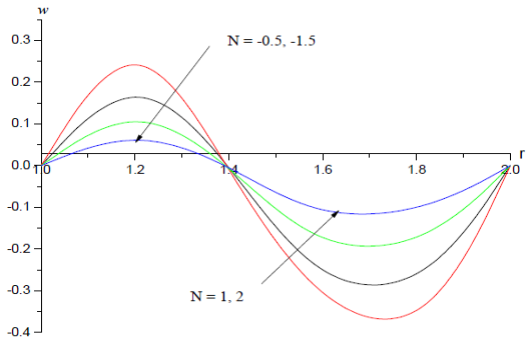


Fig. 6 Effect of  $w$  with  $N$   
 $G=10, M=0.5, D^1=2, \alpha=2, Sc=1.3,$   
 $Q1=0.5, Rd=0.5, \gamma=0.5, \lambda_1=0.1, \gamma_1=0.1$

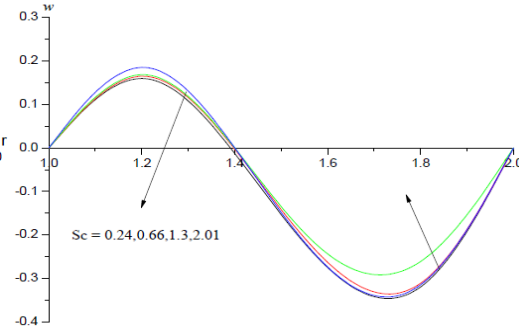


Fig. 7 Effect of  $w$  with  $Sc$   
 $G=10, M=0.5, D^1=2, \alpha=2, N=1,$   
 $Q1=0.5, Rd=0.5, \gamma=0.5, \lambda_1=0.1, \gamma_1=0.1$

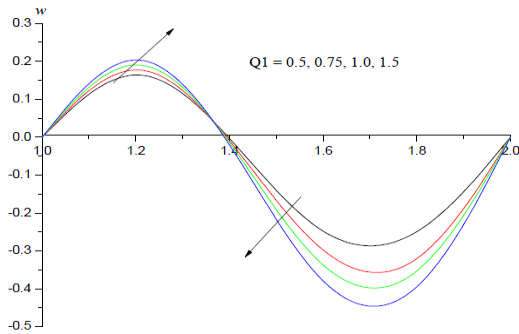


Fig. 8 Effect of  $w$  with  $Q1$   
 $G=10, M=0.5, D^1=2, \alpha=2, N=1, Sc=1.3,$   
 $Rd=0.5, \gamma=0.5, \lambda_1=0.1, \gamma_1=0.1$

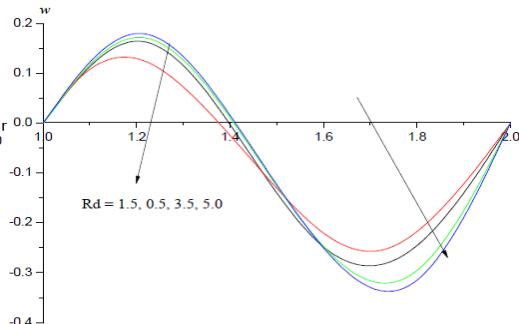


Fig. 9 Effect of  $w$  with  $Rd$   
 $G=10, M=0.5, D^1=2, \alpha=2, N=1, Sc=1.3,$   
 $Q1=0.5, \gamma=0.5, \lambda_1=0.1, \gamma_1=0.1$

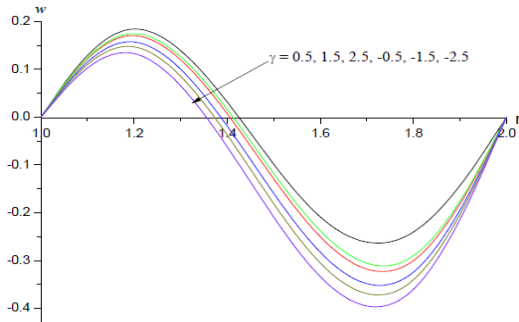


Fig. 10 Effect of  $w$  with  $\gamma$   
 $G=10, M=0.5, D^1=2, \alpha=2, N=1, Sc=1.3,$   
 $Q1=0.5, Rd=0.5, \lambda_1=0.1, \gamma_1=0.1$

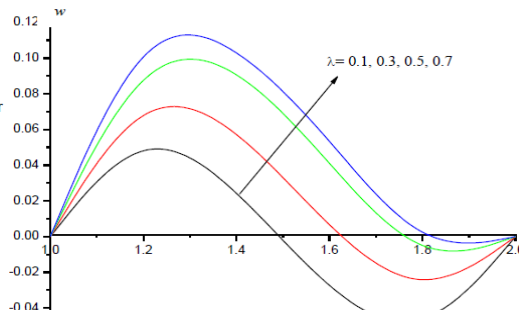


Fig. 11 : Variation of  $w$  with  $\lambda$   
 $Q1=0.5, N=1, \gamma=0.5, Sc=1.3, \alpha=2, \lambda_1=0.1, \gamma_1=0.1$

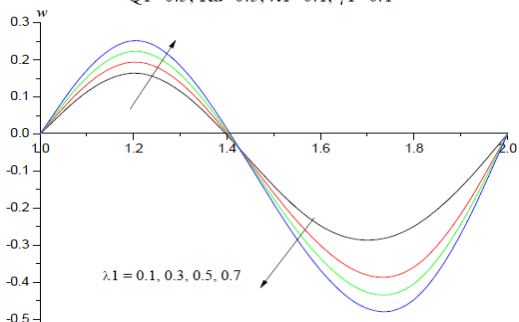


Fig. 12 Effect of  $w$  with  $\lambda_1$   
 $G=10, M=0.5, D^1=2, \alpha=2, N=1, Sc=1.3,$   
 $Q1=0.5, Rd=0.5, \gamma=0.5, \gamma_1=0.1$

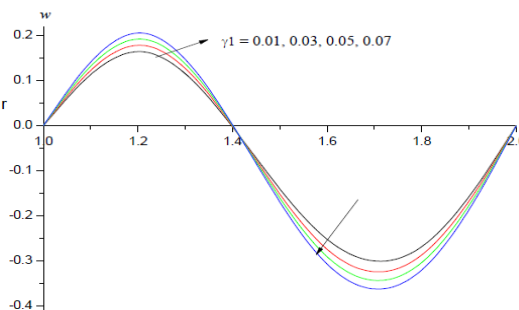


Fig. 13 Effect of  $w$  with  $\gamma_1$   
 $G=10, M=0.5, D^1=2, \alpha=2, N=1, Sc=1.3,$   
 $Q1=0.5, Rd=0.5, \gamma=0.5, \lambda_1=0.1$

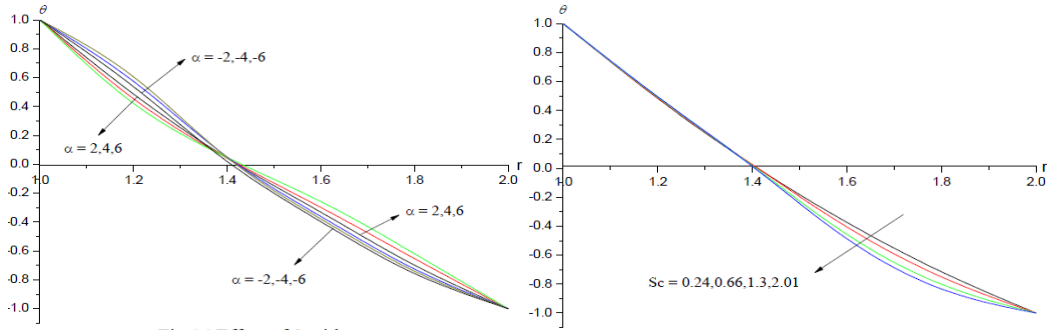


Fig.14 Effect of  $\theta$  with  $\alpha$   
 $Sc=1.3, Q1=0.5, Rd=0.5, \gamma=0.5, \lambda1=0.1, \gamma1=0.1$

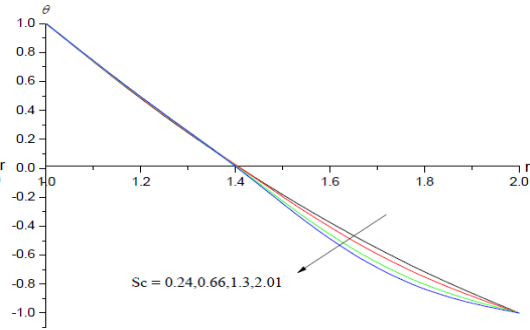


Fig.15 Effect of  $\theta$  with  $Sc$   
 $\alpha=2, Q1=0.5, Rd=0.5, \gamma=0.5, \lambda1=0.1, \gamma1=0.1$

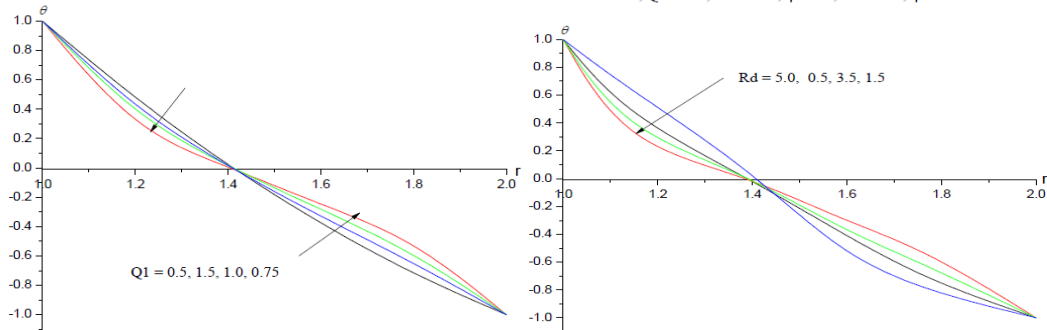


Fig.16 Effect of  $\theta$  with  $Q1$   
 $G=10, M=0.5, D^1=2, \alpha=2, N=1, Sc=1.3, Rd=0.5, \gamma=0.5, \lambda1=0.1, \gamma1=0.1$

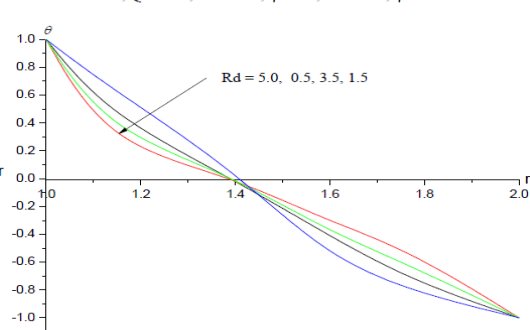


Fig.17 Effect of  $\theta$  with  $Rd$   
 $G=10, M=0.5, D^1=2, \alpha=2, N=1, Sc=1.3, Q1=0.5, \gamma=0.5, \lambda1=0.1, \gamma1=0.1$

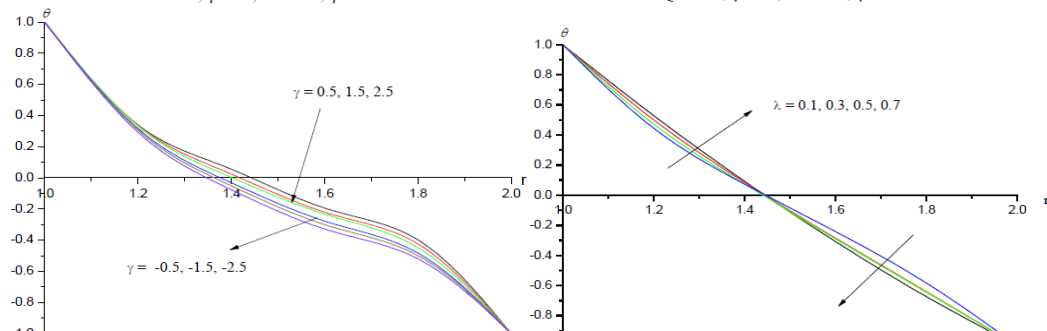


Fig.18 Effect of  $\theta$  with  $\gamma$   
 $G=10, M=0.5, D^1=2, \alpha=2, N=1, Sc=1.3, Q1=0.5, Rd=0.5, \lambda1=0.1, \gamma1=0.1$

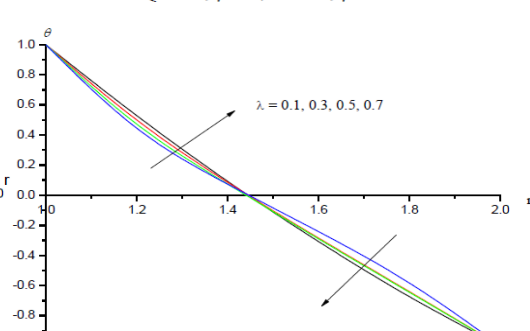


Fig. 19 : Variation of  $\theta$  with  $\lambda$   
 $Q1=0.5, Sc=1.3, \gamma=0.5, \alpha=2, \lambda1=0.1, \gamma1=0.1, Rd=0.5$

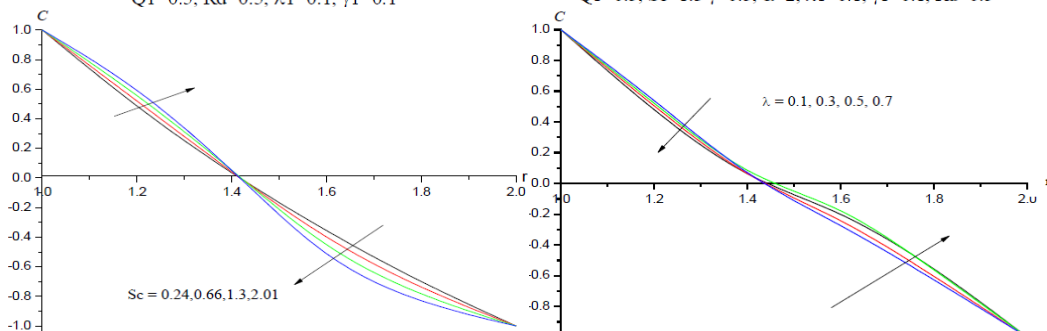


Fig.20 Effect of  $C$  with  $Sc$   
 $\gamma=0.5, \lambda=0.1$

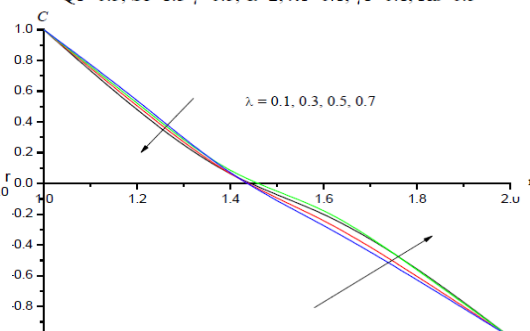


Fig. 21 : Variation of  $C$  with  $\lambda$   
 $Sc=1.3, \gamma=0.5$

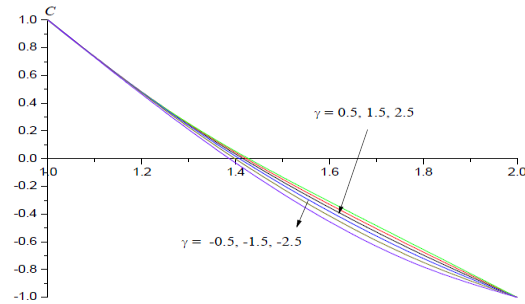


Fig.22 Effect of C with  $\gamma$   
 $Sc=1.3, \lambda=0.1$

Table : 2 – Shear Stress ( $\tau$ ), Nusselt Number (Nu) and Sherwood Number (Sh) at  $r = 1 \& 2$

Parameter		$\tau(1)$	$\tau(2)$	Nu(1)	Nu(2)	Sh(1)	Sh(2)
G	10	3.15783	2.85564				
	20	6.32324	5.69929	----	----	----	----
	30	9.52628	8.50498				
M	2	3.15783	2.85564				
	5	2.44232	2.53238	----	----	----	----
	10	1.45146	1.85790				
D-1	0.2	3.15783	2.85564				
	0.4	3.05828	2.73992	----	----	----	----
	0.6	2.96403	2.63691				
N	1.0	3.15783	2.85564				
	2.0	4.58336	4.41584	----	----	----	----
	-0.5	0.99977	0.52610				
	-1.5	0.57319	0.57212				
Sc	0.24	3.10364	2.91074	-2.17420	-1.66190	-2.87915	-1.14345
	0.66	3.12206	2.89203	-2.17308	-1.66298	-2.84527	-1.17750
	1.3	3.15783	2.85564	-2.17092	-1.66508	-2.78057	-1.24360
	2.01	3.19428	2.81828	-2.16871	-1.66724	-2.71527	-1.31129
Rd	0.5	3.15783	2.85564	-2.17092	-1.66508		
	1.5	3.15902	2.84599	-2.18364	-1.69411		
	3.5	3.15971	2.83893	-2.19354	-1.71577		
	5.0	3.16008	2.83643	-2.19664	-1.72316		
$\alpha$	2.0	3.15783	2.85564	-2.17092	-1.66508		
	4.0	3.15597	2.84853	-2.19130	-1.69160		
	6.0	3.15407	2.84153	-2.13036	-1.61105		
	-2.0	3.16082	2.87070	-2.10983	-1.58379		
	-4.0	3.16257	2.87815				
	-6.0	3.16428	2.88574				
Q1	0.5	3.15783	2.85564	-2.17092	-1.66508		
	1.0	3.17411	2.89383	-2.03128	-1.51441		
	1.5	3.19061	2.93178	-1.89129	-1.36401		
	2.0	3.24567	3.01234	-1.75132	-1.21358		
$\gamma$	0.5	3.15783	2.85564	-2.17092	-1.66508	-2.78057	-1.24360
	1.5	6.35881	5.55567	-2.16977	-1.66879	-2.86409	-1.43095
	2.5	7.18696	6.72099	-2.16902	-1.67199	-2.95321	-1.60475
	-0.5	3.13164	2.93900	-2.17257	-1.66074	-2.70462	-1.04032
	-1.5	3.09255	3.03843	-2.17532	-1.65529	-2.64127	-0.81644
	-2.5	3.03740	3.15832	-2.17654	-1.64897	-2.62143	-0.61328
$\lambda$	0.1	3.15783	2.85564	-2.17092	-1.66508	-2.78057	-1.24360
	0.2	3.89672	1.98791	-1.12475	-2.99130	-2.54760	-1.49169
	0.3	4.56571	1.02245	-0.33708	-4.51743	-2.32919	-1.74170
	0.5	5.07097	0.08511	0.18912	-6.15156	-2.12478	-1.99357
$\gamma_1$	0.01	3.15783	2.85564				
	0.02	3.19015	2.83296				
	0.03	3.22245	2.81028	----	----	----	----
	0.05	3.25475	2.78761				
$\lambda_1$	0.1	3.15783	2.85564	-2.17092	-1.66508		
	0.3	3.66965	3.33470	-2.16856	-1.66659		
	0.5	4.06164	3.86937	-2.16595	-1.66825		
	0.7	4.64804	4.25826	-2.16313	-1.67005		



## 6. CONCLUSIONS

- An increase in Grashoff number ( $G$ ) increases a velocity and reduces with  $M$  and  $D^{-1}$ .
- The axial velocity ( $w$ ) increases and actual temperature, actual concentration reduces in both generating and degenerating chemical reaction case.
- Higher the radiation absorption parameter ( $Q_1$ ) larger  $|w|$  and smaller  $\theta$  in the flow region.
- $|w|$  experiences an enhancement with increasing Jeffrey parameter  $\lambda_1$ .
- Higher the suction parameter  $\lambda$  larger  $|w|$  and actual temperature in the flow region.
- An increase in the density ratio  $\gamma_1$  results in an enhancement in a velocity.
- An increase in  $\lambda_1$  enhances  $|\tau|$  at the both cylinder.
- Higher the radiation ( $R_d$ ) larger  $|\tau|$  at  $r=1$  and smaller at  $r=2$ . The rate of heat transfer increases with  $R_d$  at both cylinders.

## 7. REFERENCES

- [1]. Abel. M. S and Mahesha. N; Heat transfer in MHD viscoelastic fluid flow over a stretching sheet with variable thermal conductivity, non-uniform heat source and radiation, Applied Mathematical Modelling, 2008, 32(10), pp. 1965–1983.
- [2]. Andersson. H. I; Slip flow past a stretching surface, ActaMechanica, 2002, 158(1-2), pp. 121-125.
- [3]. Antonio Barletle: Combined forced and free convection with viscous dissipation in a vertical duct., Int.J.heat and mass transfer, Vol.42, PP.2243-2253, (1999).
- [4]. Bhargava, R, Agarwal, R.S: Ind. J. pure and Appl. Maths, Vol.10(3), PP. 357 (1979).
- [5]. Chaudhary. S and Kumar.P; MHD slip flow past a shrinking sheet, Appl. Math, 2013, 4(3), pp. 574-581.
- [6]. Chen, T.S, Yuh, C.F : Combined heat and mass Transfer in natural convection on inclined surface. J.Heat transfer. V.2. pp.233-350, (1979).
- [7]. Datta, N : Acta Mechanica, (1977).
- [8]. Ganapathy.R, Purushothama R: Fluid flow induced by a travelling transverse wave in a saturated porous medium., J.Ind.Inst.Sci, Vol.70, PP.333 - 340 (1990).
- [9]. Gilpin, R.R: Cooling of horizontal cylinder of water through its maximum density point at 4oC, Int. J. Heat and Mass Transfer, Vol.18, p.1307, (1975).
- [10]. Goren S.L. : On free convection in water at 4oC., Chem. Engg. Sci. Vol.21, PP.515 (1966).
- [11]. Govindarajulu, J : Chem. Engng. Sci, Vol.25, PP. 18-27, (1970)
- [12]. Gupta. M, Dubey G.K, Sharma, H.S: laminar free convection flow with and without heat sources through co-axial circular pipes, Indian Jour. Pure appl. Maths. Vol.10(7), PP.792, (1979).
- [13]. Hsiao. K. L; MHD Mixed Convection for Viscoelastic Fluid Past a Porous Wedge, Int. J. Non-LinearMech, 2011, 46(1), pp. 1-8.
- [14]. Labropulu. F and Li.D; Stagnation-point flow of a second-grade fluid with slip, International Journal of Non-Linear Mechanics, 2008, 43(9), pp. 941–947.
- [15]. Mahanta .G and Shaw .S; 3D Casson fluid flow past a porous linearly stretching sheet with convective boundary condition, Alexandria Eng J, 2015, 54, 653–659.
- [16]. Madhusudhana Reddy Y : Effect of Radiation Absorption on Convective Heat and Mass Transfer Flow of Jeffrey Fluid in Concentric Cylindrical Annulus with Non – Linear Density Temperature in the Presence of Heat Source, Acceptance for Publication in Compliance Engineering Journal, December-2020.
- [17]. Ming Shen, Fei Wang and Hui Chen; MHD mixed convection slip flow near a stagnation-point on a nonlinearly vertical stretching sheet, 2015, 78, 1-15. DOI 10.1186/s13661-015-0340-6.
- [18]. Muthuchumaraswamy.R and Visalakshi; Radiative flow past an exponentially accelerated vertical plate with uniform mass diffusion, Annals of faculty engineering Hunedoara, Int Journal of engineering, 2011, IX, 137-140.
- [19]. Nanda.R.S, Purushottam . R: Int. Dedication seminar on recent advances on maths and application, Varanasi (1976).
- [20]. Neeraja.G: Ph.D. thesis, S.P. Mahila University , Tirupathi, India (1993).
- [21]. Osterle.J.F. and Young F.J.: J fluid Mechanics Vol 11.PP. 152 (1961).
- [22]. Philip.J.R.: Axisymmetric free convection at small Rayleigh number in porous cavities. Int.J.Heat and mass transfer, Vol.25.PP.1689-1699, (1982).
- [23]. Ramachandran. N, Chen. T. S and Armaly. B. F; Mixed convection in stagnation flows adjacent to vertical surfaces, ASME Journal of Heat Transfer, 1988, 110(2), pp. 373–377.
- [24]. Roots. G.: Int .J.Heat and mass transfer, Vol3.PP.1,(1961).
- [25]. Rosca. A. V and Pop. I; Flow and heat transfer over a vertical permeable stretching/shrinking sheet with a second order slip, International Journal of Heat and Mass Transfer, 2013, 60(1) pp. 355–364.
- [26]. Sarojamma. G: Ph.D. Thesis, S. K University, Anantapur, (1981).
- [27]. Sastry .V.U.K, Vajravelu, K.V : J.Fluid Mech. Vol.86, PP.365-383 (1978).

- [28]. Singh K.R., Cowling .T. J : Q.J. Maths Appl.Maths, Vol.16, PP.1,(1963).
- [29]. Sinha, P.C: Chem. Engg. Sci, Vol.24, PP. 33,(1969).
- [30]. Soundalgekar, V.M. Chem. Engg. Sci, Vol.28, PP.307,(1973).
- [31]. Sreenath.S, J.Prakash., E.Sudhakara: MHD free Convective flow of a Jeffery fluid between two coaxial impermeable and permeable cylinders, Int. J. E. IM,Vol.4, No.2,PP.13-22, (July 2012).
- [32]. Srinivas. S and Muthuraj. R; Effects of thermal radiation and space porosity on MHD mixed convection flow in a vertical channel using homotopy analysis method, Communications in Nonlinear Science and Numerical Simulation, 2010, 15(8), 2098-2108, <https://doi.org/10.1016/j.cnsns.2009.09.003>.
- [33]. Suresh Babu,V., Rajeswara Rao, U., Prasada Rao D.R.V : Effect of thermo-diffusion and chemical reaction on convective heat and mass transfer flow of a rotating micropolar fluid with Hall effect past a vertical plate. Int. J. Adv. Sci. and Tech. Research Vol.3, Issue. 4, ISSN 2249-9954, (May-June 2014).
- [34]. Varrier G.R., Tien C: Effect of Maximum density and melting on a natural convention heat transfer from a vertical plate, chem.. Engg. Proc. Sym. Sen No.82, 64, (1968).
- [35]. Vasudev .V, Rajeswara Rao .U, Subba Reddy M.V., et al., effect of Heat transfer on the peristaltic flow of jefferey fluid through a porous medium in a vertical annulus J.Basic.Appl.Sci.Res., Vol.1(7), PP.751, (2011).
- [36]. Wang. C. Y; Stagnation flows with slip: exact solutions of the Navier-Stokes equations,ZAMP, 2003, 54(1), pp. 184–189